Phonon Feedback Effects on Dynamics of Phase Slip Centers in Finite Gap Superconductors

Iris Dorn* and Armen Gulian[†]

Institute of Quantum Studies, Chapman University

Orange, California, USA

(Dated: November 22, 2021)

The results on the behavior of phase-slip centers in thin superconducting wires based on finite-element modeling and time-dependent Ginzburg-Landau (TDGL) equations are discussed. For closer relationship with experiments, we used finite-gap formulation of the TDGL system. Both the dynamic equation for the Cooper-pair condensate Ψ -function and the expression for the electric current are more complex than in the gapless case. On this basis, the influence of nonequilibrium phonons is explored. These phonons can essentially change the location of geometrical points in which the phase slippage takes place. They also affect the frequency of phase-slip oscillations. The reported effects are experimentally detectable and can be used in practical devices.

I. INTRODUCTION

The idea expressed by Bardeen, Cooper and Schrieffer in their microscopic explanation of superconductivity [1], that the Ψ -function of the Ginzburg-Landau theory [2] at thermodynamic description of superconducting state, may be related to the energy gap in the spectrum of paired electrons was proven by Gor'kov [3]. This proof elevated the phenomenological Ginzburg-Landau equations to the status of microscopic theory: for the BCS-type superconductors, such as NbTiN [4, 5], the application of GL-equations is completely adequate to the microscopic approach, at least at temperatures not far from the critical temperature T_c of the superconductor. Applicability of the phonon model to objects such as cuprates or iron-based superconductors is still being debated. However, phase-slip centers (PSCs) have been detected in high-temperature cuprate superconductors decades ago [6]. If the described properties in this report of the phase-slip centers would be found in these materials as well, that will shed additional light onto the current unknowns and help with understanding the puzzling mechanism of superconductivity in these materials.

The generalization of GL-equations for time-dependent problems took considerable effort. The first successful step was by Schmid [7], who came to the conclusion that the proper equation for the Ψ -function is not like the Schrdinger's one, but rather has a structure similar to the diffusion equation. Later, this result was confirmed by liashberg and Gor'kov [8, 9], on the basis of the Green's functions approach to superconductivity. Interestingly at that point, a closed system of TDGL equations resulted for gapless superconductors only [10]. After the development of a more powerful energy-integrated Green's functions technique for the kinetic equations in nonequilibrium superconductors, the TDGL set of equations was derived for finite gap superconductors [11–15].

The first dynamic equation is for the order parameter $\Delta = |\Delta| \exp(i\theta)$:

$$-\frac{\pi}{8T_c} \frac{1}{\sqrt{1 + (2\tau_{\varepsilon}|\Delta|)^2}} \left(\frac{\partial}{\partial t} + 2i\varphi + 2\tau_{\varepsilon}^2 \frac{\partial|\Delta|^2}{\partial t} \right) \Delta + \frac{\pi}{8T_c} \left[D(\nabla - 2i\mathbf{A})^2 \right] \Delta + \left[\frac{T_c - T}{T_c} - \frac{7\zeta(3)|\Delta|^2}{8(\pi T_c)^2} + P(|\Delta|) \right] \Delta = 0 \quad (1)$$

Here the theoretical units $\hbar = c = e = 1$ are used, **A** and φ are the vector and scalar potentials of the electromagnetic field, τ_{ε} is the electron-phonon relaxation time, D is the electronic diffusion coefficient, $\zeta(3)$ is the Riemann zeta function, and $P(|\Delta|)$ is the nonequilibrium phonon term which will be specified below (in absence of the phonon feedback $P(|\Delta|) = 0$). The order parameter Δ $(|\Delta|)$ is the superconducting energy gap), as was mentioned above, is proportional to the original Ginzburg-Landau Ψ -function (normalized so as its squared modulus is equal to the density of pair condensate). Equation (1) describes the behavior of the Cooper-pair condensate, taking into account inelastic electron-phonon collisions. In case of very strong inelastic collisions $(\tau_{\varepsilon} \to 0)$, Eq.(1) converts into its gapless form [8], where the relaxation of Δ takes place only due to the condensate itself.

The second equation in the system of GL-equations is for the electric current density, \mathbf{j} . In the static case, the electric field, $\mathbf{E} = -\dot{\mathbf{A}} - \nabla \varphi$, cannot exist in superconductors, so that the current contains only the superfluid motion of pairs: $\mathbf{j} = \mathbf{j}_s[\pi \sigma_n |\Delta|^2/(4T)]\mathbf{Q}$, where $\mathbf{Q} = -2\mathbf{A} + \nabla \theta$. In the dynamic case, the current was initially presented in the form which corresponds to the two-fluid model of superconductivity [16]: $\mathbf{j} = \mathbf{j}_s + \mathbf{j}_n$, where $\mathbf{j}_n = \sigma_n \mathbf{E}$ (σ_n is the conductivity of normal excitations in the superconductor). Later, it was shown in [17] that, for the finite gap superconductors, the microscopic theory yields additional terms in the current and this corresponds to the interference between superconducting and normal motions of electrons. Thus the

^{*} irdorn@chapman.edu

[†] gulian@chapman.edu

current expression adequate to (1) is:

$$\mathbf{j} = \mathbf{j}_{s} + \mathbf{j}_{n} + \mathbf{j}_{int} = \frac{\pi \sigma_{n}}{4T} \mathbf{Q} \left(|\Delta|^{2} - 2\tau_{\varepsilon} \frac{\partial |\Delta|^{2}}{\partial t} \right) + \sigma_{n} \mathbf{E} \left(1 + \frac{|\Delta|}{2T} \frac{\sqrt{1 + (2\tau_{\varepsilon}|\Delta|)^{2}}}{2\tau_{\varepsilon}|\Delta|} \right) \times \left[K \left(\frac{2\tau_{\varepsilon}|\Delta|}{\sqrt{1 + (2\tau_{\varepsilon}|\Delta|)^{2}}} \right) - E \left(\frac{2\tau_{\varepsilon}|\Delta|}{\sqrt{1 + (2\tau_{\varepsilon}|\Delta|)^{2}}} \right) \right] \right).$$
(2)

Here K(x) and E(x) are the complete elliptic integrals of the first and second kind, respectively. Since $[K(x) - E(x)]/x \to 0$ at $x \to 0$, one can recognize that, as in the case of (1) at $\tau_{\varepsilon} = 0$, (2) yields the gapless limit. With these interference terms included into the expression for the current, the system of TDGL equations (1) and (2) acquires a similar level of accuracy and should be used for the quantitative description of the dynamics for finite gap superconductors.

The major issue of interest in this article is the phonon feedback, for which task we need to specify the function $P(|\Delta|)$ in (1). As shown in [17, 18], this function has a form:

$$P(|\Delta|) = -2\tau_{\varepsilon} \operatorname{Re} \int_{0}^{\infty} d\varepsilon \frac{\Gamma(\varepsilon)}{\sqrt{(\varepsilon + i\gamma)^{2} - |\Delta|^{2}}}, \quad (3)$$

where $\gamma = (2\tau_{\varepsilon})^{-1}$. $\Gamma(\varepsilon)$ is related with the nonequilibrium population of phonons $\delta N_{\omega_{\alpha}}$ via:

$$\Gamma(\varepsilon) = \frac{\pi \lambda}{2(up_F)^2} \int_0^\infty \omega_{\mathbf{q}}^2 d\omega_{\mathbf{q}} \int_{|\Delta|}^\infty d\varepsilon' \delta(\varepsilon' + \varepsilon - \omega_{\mathbf{q}}) \times (u_\varepsilon u_{\varepsilon'} + v_\varepsilon v_{\varepsilon'}) (1 - n_\varepsilon - n_{\varepsilon'}) \delta N_{\omega_{\mathbf{q}}}.$$
(4)

In (4), λ is the dimensionless electron-phonon interaction constant, u is the speed of sound in the superconductor, p_F is the electron Fermi momentum, $\omega_{\bf q}$ denotes the frequency of a phonon with momentum ${\bf q}$, $u_\varepsilon = |\varepsilon|\theta(\varepsilon^2 - |\Delta|^2)/\sqrt{\varepsilon^2 - |\Delta|^2}$ is the BCS density of states for electrons, $v_\varepsilon = u_\varepsilon |\Delta|/\varepsilon$, and n_ε is the distribution function of nonequilibrium electrons. The nonequilibrium phonon distribution function should be found from the kinetic equation:

$$\frac{d}{dt}(\delta N_{\omega_{\mathbf{q}}}) = I(N_{\omega_{\mathbf{q}}}) + L(N_{\omega_{\mathbf{q}}}), \tag{5}$$

where $I(N_{\omega_{\mathbf{q}}})$ is the phonon-electron collision integral, and $L(N_{\omega_{\mathbf{q}}})$ is the operator describing the phonon exchange of a superconductor with its environment (the heat-bath). In the simplest approximation [18, 19], the latter may be defined as:

$$L(N_{\omega_q}) \approx -\frac{\delta N_{\omega_{\mathbf{q}}}}{\tau_{\mathrm{es}}} \,,$$
 (6)

where $\tau_{\rm es} = \alpha d/s$ is the phonon escape time (into the heat-bath), d is the characteristic dimension of the superconductor (e.g., thickness of the film), s is the speed of sound in it, and $0 < \alpha < 1$ is a numeric factor typically more than unity [20]. If $\tau_{\rm es} \to 0$, the phonons are in equilibrium, $\delta N_{\omega_{\mathbf{q}}} \to 0$. However, in many practically important cases, $\tau_{\rm es}$ is finite and (5) should be solved jointly with (1) and (2). In the so-called "generalized local equilibrium approximation", the solution for δN_{ω_0} is obtained in [21, 22]. Rather than using this solution, we will notice that in the absence of population inversion [23, 24], which until now has not vet been observed experimentally, the integrand in (4), as well as the function $\Gamma(\varepsilon)$ itself, are positively defined at presence of excess phonons $\delta N_{\omega_{\mathbf{q}}} > 0$. Then, after substitution of $\Gamma(\epsilon)$ into (3), we will find negatively defined function $P(|\Delta|)$.

In the first approximation, we will consider this function independent on $|\Delta|$: $P(|\Delta|) = P$ and simply vary its dimensionless value when solving the TDGL system to understand the role of this phonon term. As follows from the analysis of Eq. (1), this function effectively reduces the local value of critical temperature T_c . Its nonzero value is caused by external factors, which may have occasional character, like a film-substrate mismatch or be created deliberately by a heat deposition via various mechanisms (optical pulses, phonon sources, etc.). Thus, during modeling analysis, we may vary not only its amplitude but also its location in space and appearance in time.

II. DIMENSIONLESS EQUATIONS

For numerical analysis, it is convenient to represent the system of TDGL equations in the dimensionless form. For the dimensionless order parameter $\Psi = \Delta/\Delta_0$ (here $\Delta_0 = \{8\pi^2 T_c(T_c - T)/[7\zeta(3)]\}^{1/2}$ and $\zeta(3) \approx 1.2$ is the Riemann ζ - function) one can obtain from (1) the following dimensionless equation:

$$\frac{1}{\sqrt{1+\delta^2|\Psi|^2}} \left(\frac{\partial}{\partial \tau} + i \ \bar{\varphi} + \frac{1}{2} \delta^2 \frac{\partial |\Psi|^2}{\partial \tau} \right) \Psi$$

$$= \xi^2 (\nabla - 2i\mathbf{A})^2 \Psi + (1 - |\Psi|^2 + p) \Psi. \quad (7)$$

Here, $\delta = 2\tau_{\varepsilon}\Delta_{0}$, $\tau = tD/\xi^{2} \equiv t/t_{0}$, $\bar{\varphi} = 2\varphi\xi^{2}/D \equiv 2\varphi t_{0}$, $\xi \equiv \xi(T) = \{\pi D/[8(T_{c}-T)]\}^{1/2}$, where $\xi(T)$ is the "dirty metal" superconducting coherence length, and $p = T_{c}/(T_{c}-T)P(|\Delta|)$. The vector potential as well as the spatial derivatives in (7) are not yet dimensionless. The reason is that in the Ginzburg-Landau approach another spatial parameter, the London penetration length, λ_{L} , comes in from the equation for the current density \mathbf{j} (2). Using the relations curl $\mathbf{H} = 4\pi \mathbf{j} = \text{curlcurl } \mathbf{A}$, $u = \pi^{4}/[14\zeta(3)] \approx 5.798$, $\eta = (T_{c} - T)/T_{c}$, and also choosing the gauge $\varphi = 0$, we can transform (2) into:

$$\begin{split} \sigma \dot{A} \Bigg[1 + \frac{2}{\pi} \sqrt{\eta u} |\Psi| \frac{\sqrt{(|\Psi|\delta)^2 + 1}}{|\Psi|\delta} \Bigg[K \bigg(\frac{|\Psi|\delta}{\sqrt{|\Psi|^2 \delta^2 + 1}} \bigg) \\ - E \bigg(\frac{|\Psi|\delta}{\sqrt{|\Psi|^2 \delta^2 + 1}} \bigg) \Bigg] \Bigg] = \\ - \bigg[A + \frac{i}{2\kappa |\Psi|^2} (\psi^* \nabla \psi - \psi \nabla \psi^*) \bigg] \\ \times \bigg(|\Psi|^2 - 2\delta \sqrt{\frac{\eta}{u}} \frac{\partial |\Psi|^2}{\partial \tau} \bigg) - \nabla \times \nabla \times A \quad (8) \end{split}$$

where $\sigma = \sigma_n/t_0$ and $\kappa = \lambda_L/\xi$ is the Ginzburg-Landau parameter with the London penetration depth $\lambda_L = \{8\pi^4\sigma_n(T_c-T)/[7\zeta(3)]\}^{-1/2}$. Using this λ_L length, we will represent (7) in a fully dimensionless form:

$$\frac{1}{\sqrt{1+\delta^2 |\Psi|^2}} \frac{\partial \Psi}{\partial \tau} = -\frac{\delta^2}{2\sqrt{1+\delta^2 |\Psi|^2}} \frac{\partial |\Psi|^2}{\partial \tau} \Psi - \left[\left(\frac{i}{\kappa} \nabla + A \right) \right]^2 \Psi + \left(1 - |\Psi|^2 + p \right) \Psi$$
(9)

in the same $\varphi = 0$ gauge as (8).

The elliptic integrals in (8) can be approximated by elementary functions (Fig. 1):

$$K(x) - E(x) \cong \frac{\ln(1+x) - \ln(1-x)}{2} + (1-x)\ln(1-x) \equiv \frac{\ln(1-x^2)}{2} - x\ln(1-x) \equiv f(x)/x.$$
(10)

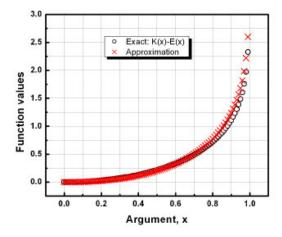


FIG. 1. Comparison of exact difference of elliptic functions and its approximation by (10).

During modeling we used both the exact value and its logarithmic approximation (10) without noticeable difference in solutions.

III. RESULTS OF MODELING

We applied (8) and (9) to a very thin superconducting wire. In this case the problem is spatially 1-dimensional. Technical details of COMSOL Multiphysics® code are discussed in Appendix A. In brief, we used General Mathematical Module with three general form PDE interface scalar functions. The complex Ψ -function is represented by $\Psi(x) = \text{Re}\,\Psi(x) + i\,\text{Im}\,\Psi(x)$ and the vector potential is described by a scalar A(x) for the 1-D problem.

The wire is arranged symmetrically at $-L \leq x \leq L$ between the massive superconducting banks. We accept $|\Psi(x=\pm L)|=1$ and $|\Psi'(x=\pm L)|=0$, the last of which imposes $(\text{Re }\Psi)'(x=\pm L)=0$, $(\text{Im }\Psi)'(x=\pm L)=0$ as boundary conditions. For the vector potential we will use the relation $A(x=\pm L)=-4\pi j_0$ which follows from (8) and the boundary conditions for the Ψ -function. This external parameter j_0 regulates the current through the wire: the current is zero when $j_0=0$.

We will begin with the discussion of the solutions in absence of the phonon term, p=0. When the current exceeds the critical value (in case of Fig. 2: $j_0=0.4$ for $\Delta=0.1$), the temporal oscillations begin, with $|\Psi|^2$ touching zero periodically at the middle of the wire.

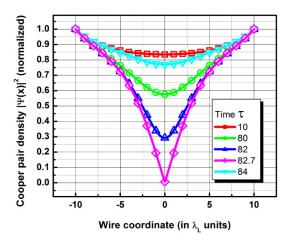


FIG. 2. Spatial distribution of wave-function modulus at different moments of time for critical current, $j_0 = 0.4$ and $\Delta = 0.1$ without phonon term, p = 0.

This behavior of PSCs in 1D wires has been extensively studied in the literature both experimentally and theoretically (to name a few, see [14, 15, 25–31], as well as the review articles and books:[21, 22, 32–35] and references therein).

At this point the phonon term, p(x,t) with spatial width 0.1 (this size is used for all the examples considered

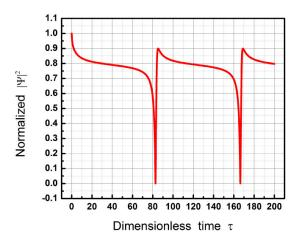


FIG. 3. Temporal behavior of $|\Psi|$ at the middle of the wire, x = 0, for critical current, $j_0 = 0.4$ and $\Delta = 0.1$ without phonon term, p = 0

further on), may be brought in and that will introduce new features and results. As was explained in Section 1, in case of positive phonon fluxes (hot spots with elevated temperature along the wire) p should have negative values. We will start with non-zero p located at the middle of the wire. Then as described in Fig. 4, the PSC oscillations may occur at under-critical values of j_0 . This is

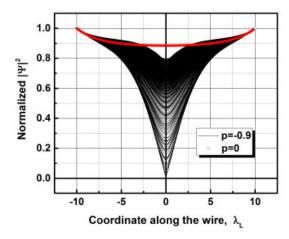
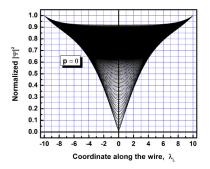
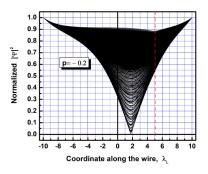


FIG. 4. At p=0 and $j_0=0.37$ there are no oscillations; $|\Psi|$ is just sagging as shown. At p=-0.9 oscillations are present. In both cases $\Delta=0.1$.

not surprising because in addition to "weakness" at the center of the wire caused by the symmetry, the p-term is adding an additional "weakness" via elevation of "effective" temperature. It is less obvious what will happen when the location of the p-term is shifted from the central position. To explore, we located it at x = 5. Very interestingly, in this case the actual position at which $|\Psi|^2$

is touching zero is determined in competition of "geometrical weakness" (i.e., x=0) with "thermal weakness" (i.e., x=5). The higher the |p|, the closer the touching point to the location of p. In Fig. 5, we described this finding by showing the spatial distribution of temporal variation of $|\Psi|^2$ for increasingly higher values of |p|.





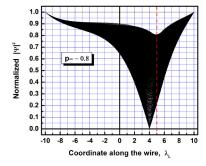
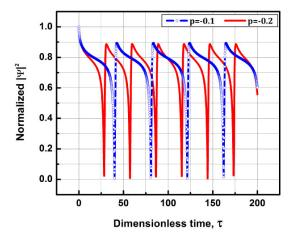


FIG. 5. Spatial distribution of Cooper pair density for different intensities of phonon flux action at established periodic PSC oscillations. $j_0 = 0.4$ and $\Delta = 0.1$. Noticeably, at the beginning of oscillations period, the sagging starts at the point where the phonon source is located. At further evolution, the sagging moves towards the geometrical center of the wire. The hotter the phonon spot is, the closer the location the phase slippage is to it.

Another remarkable feature which the phonon source is introducing is the dependence of the oscillation frequency on the intensity of the phonon hot-spot, Fig 6.

This observation constitutes the main result of our research. Since the frequency of oscillations can be measured with high accuracy, this effect may constitute a basis for high-sensitivity single-particle or radiation de-



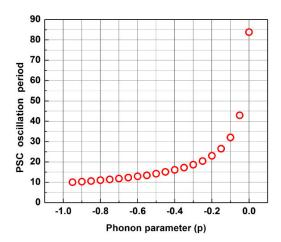


FIG. 6. Increase of |p| reduces the period of PSC oscillations.

tectors. Indeed, at the absorption of external energy. in the form of photons or other quanta, the hot-spot is occurring in the substrate which holds the wire. If the wire is biased by an under-critical current, there are no PSC oscillations. As soon as the hot-spot is created, oscillations will start with the frequency proportional to the temperature excursion caused by the event. One of the ways to detect this effect is to measure the voltage between the ends of the wire. Conversion of supercurrent into a normal current and back, which takes place during the oscillation cycle of PSC, generates the oscillations of the electric vector E along the wire. Its spatial integral yields oscillatory voltage $V(t) = \int E(t) dl$, which could be measured at the ends of the wire at the constant applied current j_0 , Fig. 7.

Though the frequency measurements are the most accurate and possess all the required information about the hot-spot, that is not the only possible measurement. A simpler measurement may suffice. The matter is the voltage, as seen from Fig. 7, is unipolar and its average value

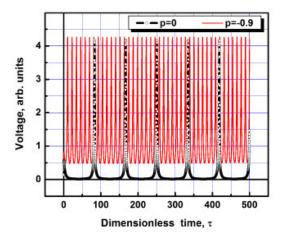


FIG. 7. Voltage vs. time across the 1D wire when PSC oscillations take place with small (p=0) and high (p=-0.9, located at the center of the wire) frequencies. Parameters are $\Delta=0.1$ and $j_c=0.4$.

is non-zero. Moreover, at higher frequencies of oscillation the average value is larger. The average values of voltage for the cases shown in Fig. 7 are $\widetilde{V}_{high\ frequency}=1.34$ and $\widetilde{V}_{low\ frequency}=0.17$. Thus, the hot spots can be characterized with high accuracy by a simple DC voltage measurement.

IV. DISCUSSION

The effects explored above have been associated with non-zero values of the phonon feedback term p. We have considered the simplest case when the non-zero values of p were caused by external sources such as the hot-spots induced by a laser or an external phonon flux. A nonequilibrium superconductor itself provides a more sophisticated origin of the p-term. For example, as we described above, during the process of phase slippage the supercurrent is transformed into a normal one. Normal current is dissipative and generates excess phonons. In Section 1, we introduced the phonon escape time, $\tau_{\rm es} = \alpha d/u$. If this time is longer than the phonon-electron relaxation time, then these nonequilibrium phonons may have an influence on the electrons. This is not the only mechanism. As was shown in [36], breaking and recombination of Cooper pairs creates correspondingly negative and positive phonon fluxes: $p \propto -\partial (|\Psi|^2)/\partial t$. Thus, the phase slip centers themselves can serve as a source of excess phonons. This nonlinear nonequilibrium mechanism requires additional theoretical investigation which is beyond the scope of this paper.

In previous literature, analogies between Josephson junctions (JJs), or, more generally, between weakly-coupled superconductors and PSC have been outlined. Continuing this analogy, we found here that due to the

phonon feedback, the nanowires with phase-slip centers possess features which can be used for detection purposes. Another aspect of the JJ - PSC analogy is related with the presence of interference current which we took into account in our computational scheme. This current is additional to the normal and the superconducting currents usually used at the TDGL description of PSCs. We used it for a more proper quantitative description of nonequilibrium effects without accentuating on its role. However, in the JJ theory there is a paradox of interference current which may reveal itself in 1D nanowires as well. Future explorations of the role of the interference current may deliver new discoveries.

V. CONCLUSIONS

Based on the TDGL equations for the finite gap superconductors, we explored dynamics of PSCs in 1D nanowires. These equations also contain the term responsible for the action of nonequilibrium phonons on the order parameter in the superconductor. Excess nonequilibrium phonons, of the internal or external origin, are affecting the location of the PSC in the wire. Moreover, they affect very strongly the frequency of the PSC oscillations. This effect, discovered and described in detail in our report, may serve as a basis for practical devices, for example: particle/photon detectors. Moreover, it has a deep analogy with exponential increase of PSC oscillation frequency described by Golubev and Zaikin [37] which are in accordance with experimental findings of Bezryadin et al. [38]. The unipolar voltage at the phase-slip oscillations allows us to suggest a simple DC measurement for detecting the dynamic effect without necessity of sophisticated measurement tools for high-frequency signal acquisition. The effect can be used for the PSC single photon or particle detector (determining the color of the incident photon or the energy of the absorbed particle). In a more general sense, the phonon feedback may be influential in various superconducting electronic devices.

ACKNOWLEDGMENTS

This work was supported by the ONR Grants N00014-16-1-2269, N00014-17-1-2972, N00014-18-1-2636, and N00014-19-1-2265.

Appendix A: APPENDIX

The General Form of Mathematics Module of COM-SOL 5.5 was used with the Time Dependent Study Partial Differential Equation (PDE) interface for this simulation. The real and imaginary parts of the order parameter are represented as $\psi_1 \equiv \text{Re}(\psi) = u_1(x,t) \equiv u$ and $\psi_1 \equiv \text{Im}(\psi) = u_2(x,t) \equiv u_2$. After separation of real and imaginary parts of Ψ -function, Eq. (9) can be represented as:

$$\dot{\psi}_{1} = \frac{1 + \delta^{2}\psi_{2}^{2}}{k^{2}\sqrt{1 + \delta^{2}(\psi_{1}^{2} + \psi_{2}^{2})}} (\psi_{1.xx} + \psi_{1.yy})$$

$$- \frac{\delta^{2}\psi_{1}\psi_{2}}{k^{2}\sqrt{1 + \delta^{2}(\psi_{1}^{2} + \psi_{2}^{2})}} (\psi_{2.xx} + \psi_{2.yy})$$

$$+ \frac{2(1 + \delta^{2}\psi_{2}^{2})}{k\sqrt{1 + \delta^{2}(\psi_{1}^{2} + \psi_{2}^{2})}} (A\psi_{2.x})$$

$$+ \frac{2\delta^{2}\psi_{1}\psi_{2}}{k\sqrt{1 + \delta^{2}(\psi_{1}^{2} + \psi_{2}^{2})}} (A\psi_{1.x})$$

$$+ \frac{\psi_{2}\sqrt{1 + \delta^{2}(\psi_{1}^{2} + \psi_{2}^{2})}}{k} (A_{.x})$$

$$- \frac{\psi_{1}}{\sqrt{1 + \delta^{2}(\psi_{1}^{2} + \psi_{2}^{2})}} A^{2} + \frac{\psi_{1}(1 - \psi_{1}^{2} - \psi_{2}^{2} - 2\mu^{2} + p)}{\sqrt{1 + \delta^{2}(\psi_{1}^{2} + \psi_{2}^{2})}} (A_{1})$$
(A1)

$$\dot{\psi}_{2} = \frac{1 + \delta^{2}\psi_{1}^{2}}{k^{2}\sqrt{1 + \delta^{2}(\psi_{1}^{2} + \psi_{2}^{2})}} (\psi_{2.xx} + \psi_{2.yy})$$

$$- \frac{\delta^{2}\psi_{1}\psi_{2}}{k^{2}\sqrt{1 + \delta^{2}(\psi_{1}^{2} + \psi_{2}^{2})}} (\psi_{1.xx} + \psi_{1.yy})$$

$$- \frac{2(1 + \delta^{2}\psi_{1}^{2})}{k\sqrt{1 + \delta^{2}(\psi_{1}^{2} + \psi_{2}^{2})}} (A_{1}\psi_{1.x})$$

$$- \frac{2\delta^{2}\psi_{1}\psi_{2}}{k\sqrt{1 + \delta^{2}(\psi_{1}^{2} + \psi_{2}^{2})}} (A\psi_{2.x})$$

$$- \frac{\psi_{1}\sqrt{1 + \delta^{2}(\psi_{1}^{2} + \psi_{2}^{2})}}{k} (A_{.x})$$

$$- \frac{\psi_{2}}{\sqrt{1 + \delta^{2}(\psi_{1}^{2} + \psi_{2}^{2})}} A^{2} + \frac{\psi_{2}(1 - \psi_{1}^{2} - \psi_{2}^{2} - 2\mu^{2} + p)}{\sqrt{1 + \delta^{2}(\psi_{1}^{2} + \psi_{2}^{2})}} (A_{2})$$
(A2)

The vector potential A, Eq. 8, was represented by $u3(x,t) \equiv u3$. Its equation has the form:

$$\sigma \dot{A} \left(1 + \frac{2}{\pi} \sqrt{\eta * 5.798} |\psi| \frac{\sqrt{(|\psi|\delta)^2 + 1}}{|\psi|\delta} \right)$$

$$\times \left[K \left(\frac{|\psi|\delta}{\sqrt{|\psi|^2 \delta^2 + 1}} \right) - E \left(\frac{|\psi|\delta}{\sqrt{||\psi|^2 \delta^2 + 1}} \right) \right] \right)$$

$$= - \left[A + \frac{(\psi_2 \nabla \psi_1 - \psi_1 \nabla \psi_2)}{\kappa |\psi|^2} \right]$$

$$\times \left(|\psi|^2 - 2\delta \sqrt{\frac{\eta}{5.798}} \frac{\partial |\psi|^2}{\partial \tau} \right) - j_0 \quad (A3)$$

where $|\psi| = \sqrt{\psi_1^2 + \psi_2^2}$, and $j_0 = 4\pi \times (current\ density)$.

Partial derivatives u_t , u_x and u_{xx} with respect to t and x are denoted correspondingly as ut, ux, and uxx, and similarly for u2 and u3. The form of the PDE to be

solved is:

$$d_a = \sigma [1 + (1/\pi)(5.798 \cdot \eta(u^2 + u_2^2))^{1/2}] \times [exact(1/(1 + 1/((u^2 + u_2^2)\delta^2))^{1/2})], \quad (A4)$$

where exact is an interpolated function corresponding to f(x)/x in (10) defined in the set of Global Definitions from an expression for the Interpolation function based on an imported data table of complete elliptic integrals K(x) - E(x) (since COMSOL does not have them in its internal mathematical library). Equivalently for this analytic function, we also used the logarithmic approximation from Eq. (10). The expressions for terms Γ and F for each PDE are given below. For PDE_1 :

$$\Gamma = -u_x/\kappa^2,\tag{A5}$$

$$f = -u_{xx}/\kappa^{2} + \left((1 + \delta^{2}u_{2}^{2})u_{xx} \right) / \left(\kappa^{2}\sqrt{1 + \delta^{2}(u^{2} + u_{2}^{2})} \right)$$

$$- (\delta^{2}uu_{2}u_{2xx}) / \left(\kappa^{2}\sqrt{1 + \delta^{2}(u^{2} + u_{2}^{2})} \right)$$

$$+ (2u_{2x}(1 + \delta^{2}u_{2}^{2})u_{3}) / \left(\kappa\sqrt{1 + \delta^{2}(u^{2} + u_{2}^{2})} \right)$$

$$+ (2u_{x}\delta^{2}uu_{2}u_{3}) / \left(\kappa\sqrt{1 + \delta^{2}(u^{2} + u_{2}^{2})} \right)$$

$$+ \left(u_{2}u_{3x}\sqrt{1 + \delta^{2}(u^{2} + u_{2}^{2})} \right) / \kappa$$

$$- uu_{3}^{2} / \sqrt{1 + \delta^{2}(u^{2} + u_{2}^{2})}$$

$$+ u \left(1 - u^{2} - u_{2}^{2} \right)$$

$$+ p[((x - x_{0})/2)^{2} < width] / \sqrt{1 + \delta^{2}(u^{2} + u_{2}^{2})}, \quad (A6)$$

where x_0 is the location of the phonon source, and width is its spatial width. Similarly, for PDE_2 :

$$\Gamma = -u_{2x}/\kappa^2 \tag{A7}$$

For PDE_3 :

$$\Gamma = 0 \tag{A9}$$

$$f = -u_3[u^2 + u_2^2 + 2\delta a_{11}(2uu_t + 2u_2u_{2t})] + [(uu_{2x} - u_2u_x)/\kappa] \times [1 + 2a_{11}(\delta/(u^2 + u_2^2))(2uu_t + 2u_2u_{2t})] - j_0, \quad (A10)$$

where $a_{11} = \sqrt{\eta/5.798}$. The default Neumann boundary conditions ($n \cdot \Gamma = 0$) for the functions ψ_1 and ψ_2 correspond to the ones specified in Section 3. For the vector potential Eq. (8), this equation as well the *Dirichlet boundary condition* is utilized with the *Prescribed value* $r_3 = -j_0$. In additional, initial values must be applied for each PDE interface. We used at t = 0: u = 1, $u_2 = 0$ and $u_3 = -j_0$.

At our computations we used *User-controlled mesh* with *Custom Element Size Parameters* with *Maximum element size* 0.005, *Maximum element growth rate* 1 and *Resolution of narrow regions* 1.

 $f = -u_{2xx}/\kappa^{2} + ((1 + \delta^{2}u_{2}^{2})u_{2xx}) / \left(\kappa^{2}\sqrt{1 + \delta^{2}(u^{2} + u_{2}^{2})}\right)$ $- (\delta^{2}uu_{2}u_{xx}) / \left(\kappa^{2}\sqrt{1 + \delta^{2}(u^{2} + u_{2}^{2})}\right)$ $- (2u_{x}(1 + \delta^{2}u^{2})u_{3}) / \left(\kappa\sqrt{1 + \delta^{2}(u^{2} + u_{2}^{2})}\right)$ $- (2u_{2x}\delta^{2}uu_{2}u_{3}) / \left(\kappa\sqrt{1 + \delta^{2}(u^{2} + u_{2}^{2})}\right) / \kappa$ $- \left(uu_{3x}\sqrt{1 + \delta^{2}(u^{2} + u_{2}^{2})}\right) / \kappa$ $- u_{2}u_{3}^{2} / \sqrt{1 + \delta^{2}(u^{2} + u_{2}^{2})}$ $+ u_{2}\left(1 - u^{2} - u_{2}^{2}\right)$ $+ p[((x - x_{0})/2)^{2} < width] / \sqrt{1 + \delta^{2}(u^{2} + u_{2}^{2})}.$ (A8)

J. Bardeen, L. N. Cooper, and J. R. Schrieffer, Phys. Rev. 108, 1175 (1957).

^[2] V. L. Ginzburg and L. D. Landau, Zh. Eksp. i Teor. Fiz. 20, 1064 (1950), [English translation in: L. D. Landau, Collected papers (Oxford: Pergamon Press, 1965) p. 546].

^[3] L. Gor'kov, Zh. Eksp. i Teor. Fiz. 36, 1918 (1959), [Sov. Phys. JETP 9 (1959) 1364].

^[4] Y. Ivry, C.-S. Kim, A.E.Dane, D. DeFazio, A.N.McCaughan, K.A.Sunter, Q.Zhao, and K.K.Berggren, Phys. Rev. B 90, 214515 (2014).

^[5] D. Hunt, H. G. LeDuc, S. R. Cypher, J. A. Stern, and

A. Judas, Appl. Phys. Lett. 55, 81 (1989).

^[6] R. B. Akopyan and S. G. Gevorgyan, Pis'ma Zh. Eksp. i Teor. Fiz. 52, 1255 (1990), [JETP Lett. 52 (1990) 674].

^[7] A. Schmid, Phys. Konden. Materie 5, 302 (1966).

^[8] L. Gor'kov and G. liashberg, Zh. Eksp. i Teor. Fiz. 54, 612 (1968), [Sov. Phys. JETP 27 (1968) 328].

^[9] L. Gor'kov and G. liashberg, J. Low Temp. Phys. 2, 161 (1970).

^[10] A. A. Abrikosov and L. P. Gor'kov, Zh. Eksp. i Teor. Fiz. 39, 1782 (1960), [Sov. Phys. JETP 12 (1961) 1243].

^[11] A. A. Golub, Zh. Eksp. i Teor. Fiz. 71, 314 (1976), [Sov. Phys. JETP 44 (1976) 178].

- [12] L. Kramer and R.J.Watts-Tobin, Phys. Rev. Lett. 40, 1041 (1978).
- [13] G. Schon and V. Ambegaokar, Phys. Rev. B. 19, 3515 (1979).
- [14] C.-R. Hu, Phys. Rev. B 21, 2775 (1980).
- [15] R. G. Watts-Tobin, Y. Krhenbhl, and L. Kramer, J. Low Temp. Phys. 42, 459 (1981).
- [16] C. Gorter and H. Casimir, Physica 1, 306 (1934).
- [17] A. M. Gulian, G. F. Zharkov, and G. M. Sergoyan, Zh. Eksp. i Teor. Fiz. 92, 190 (1987), [Sov. Phys. JETP 65 (1987) 107].
- [18] J. J. Chang, Nonequilibrium Superconductivity, Eds.: D. N. Langenberg and A. I. Larkin (North-Holland, Amsterdam, 1986), pp. 453-492.
- [19] J.-J. Chang and D. J. Scalapino, Phys. Rev. B 15, 2651 (1977).
- [20] Chang and Scalapino [19] suggested expression $\alpha=4/\eta$, where 4 is a geometrical factor, and η is an escape probability (a number between 0 and 1, related with the ratio of acoustic densities of adjacent materials).
- [21] A. M. Gulian and G. F. Zharkov, Nonequilibrium Electrons and Phonons in Superconductors (Kluwer Academic/Plenum Publishers, New York, 1999).
- [22] A. M. Gulian, Shortcut to Superconductivity (Springer, 2020) Chap. 7.
- [23] A. M. Gulyan and G. F. Zharkov, Zh. Eksp. i Teor. Fiz. 84, 1817 (1983), [Sov. Phys. JETP 57 (1983) 1059].
- [24] A. Gulian, R. Dulal, S. Teknowijoyo, and S. Chahid, Mod. Phys. Lett. B (2020), (In press).
- [25] D. Y. Vodolazov, F. M. Peeters, L. Piraux, S. Mátéfi-Tempfli, and S. Michotte, Phys. Rev. Lett. 91, 157001 (2003).

- [26] M. Tian, J. Wang, J. S. Kurtz, Y. Liu, M. H. W. Chan, T. S. Mayer, and T. E. Mallouk, Phys. Rev. B 71, 104521 (2005).
- [27] K. Xu and J. R. Heath, Nano Letters 8, 38453849 (2008).
- [28] M. W. Brenner, D. Roy, N. Shah, and A. Bezryadin, Phys. Rev. B 85, 224507 (2012).
- [29] D. Y. Vodolazov, Phys. Rev. B 75, 184517 (2007).
- [30] M. Vanevic and Y. V. Nazarov, Phys. Rev. Let. 108, 187002 (2012).
- [31] D. P. Lozano, S. Couet, C. Petermann, G. Hamoir, J. K. Jochum, T. Picot, E. Menndez, K. Houben, V. Joly, V. A. Antohe, M. Hu, B. Leu, A. Alatas, A. Said, S. Roelants, B. Partoens, M. Milosevic, F. Peeters, L. Piraux, J. VandeVondel, A. Vantomme, K. Temst, and M. VanBael, Phys. Rev. B 99, 064512 (2019).
- [32] S. Bose and P. Ayyub, Rep. Progr. Phys. 77, 116503 (2014).
- [33] K. Arutyunov, D. Golubev, and A. Zaikin, Superconductivity in one dimension, Phys. Rep. 464, 170 (2008).
- [34] A. Bezryadin, Superconductivity in Nanowires (John Wiley & Sons, Ltd, 2012).
- [35] B. Ivlev and N. Kopnin, Advances in Physics 33, 47 (1984).
- [36] A. M. Gulyan, G. F. Zharkov, and G. M. Sergoyan, Pis'ma v Zh. Eksp. i Teor. Fiz. 44, 331 (1986), [JETP Lett. 44 (1986), 426].
- [37] D. S. Golubev and A. D. Zaikin, Phys. Rev. B 64, 014504 (2001).
- [38] A. Bezryadin, C. N. Lau, and M. Tinkham, Nature 404, 971 (2000).